PSFC/JA-10-54

High confinement/high radiated power H-mode experiments in Alcator C-Mod and consequences for ITER Q_{DT} = 10 operation

Loarte, A.*, Hughes, J.W., Reinke, M.L., Terry, J.L., LaBombard, B., Brunner, D., Greenwald, M., Lipschultz, B., Ma, Y., Wukitch, S.J., Wolfe, S.

* ITER Organization

January 2011

Plasma Science and Fusion Center
Massachusetts Institute of Technology
Cambridge MA 02139 USA

This work was supported by the U.S. Department of Energy, Agreement No. DE-FC02-99ER54512.

High confinement/high radiated power H-mode experiments in Alcator C-Mod and consequences for ITER Q_{DT} = 10 operation

A. Loarte

ITER Organization, Route de Vinon sur Verdon, 13115 St Paul Lez Durance, France

J.W. Hughes, M.L. Reinke, J.L. Terry, B. LaBombard, D. Brunner, M. Greenwald, B. Lipschultz, Y. Ma, S Wukitch and S. Wolfe

Plasma Science and Fusion Centre, Massachusetts Institute of Technology, Cambridge, Massachusetts 02139, USA.

Abstract. Experiments in Alcator C-Mod in EDA H-modes with extrinsic impurity seeding (N_2, Ne, Ar) have demonstrated a direct correlation between plasma energy confinement and edge power flow achieving values of $H_{98} \geq 1$ for edge power flows only marginally exceeding the scaled power for access to H-mode confinement in these conditions. For lower Z impurity seeding (N_2, Ne), plasmas with high energy confinement are obtained with a radiative power fraction of 85% or larger and a reduction of the peak heat flux at the divertor by more than a factor of 5 compared to similar attached conditions. The H-mode plasmas thus achieved in Alcator C-Mod meet or exceed the requirements both in terms of divertor heat flux handling and energy confinement for ITER Q_{DT} = 10 operation and with an edge power flow only marginally above the H-mode threshold power (by 1.0 - 1.4) as expected in ITER.

1. Introduction.

The next generation of fusion devices, such as ITER, are required to operate in regimes with high energy confinement and high density in order to demonstrate high fusion power amplification. The confinement regime that fulfils the requirements for ITER with fusion amplification (Q_{DT}) Q_{DT}=10 is the H-mode regime, which is characterised by the formation of an edge transport barrier and steep power flux gradients in the plasma scrape-off layer. Access to this confinement regime requires a minimum level of input power be exceeded, the so-called H-mode threshold power, whose scaling to ITER has been derived from analysis of a multi-machine experimental database [Martin 2008]. The threshold power defined in [Martin 2008] does not include losses due to core radiation which are typically low in the L-mode plasmas preceding the H-mode. Because of the narrow width of the scrape-off layer power flux profile expected in ITER H-modes [PIPB 2007], power fluxes onto plasma facing components (PFCs) in ITER are expected to significantly exceed (by factors of 2 or more) those determined by technological limit for reliable operation of water cooled PFCs [Loarte 2008]. The required reduction of the power flux to PFCs in ITER and next step devices is proposed to be achieved by the dissipation of the power conducted/convected by the plasma along the field line by electromagnetic radiation and charge-exchange losses in the divertor region [IPB 1999]. This requires the establishment of a high density/low temperature divertor plasma in which partially ionised impurities radiate a major proportion of the incoming power exhausted from the main plasma. In these divertor conditions the electron temperature reaches values as low as a few eV and charge-exchange and recombination losses reduce the plasma particle flux and plasma pressure at the divertor target, establishing a state known as a detached divertor plasma which can be routinely achieved in divertor tokamak devices (see for instance [LaBombard 1995, Petrie 1997a, Loarte 1998]).

The high fusion gain Q_{DT} = 10 ITER operation is based on inductive 15 MA plasmas with high energy confinement (H_{98} = 1, normalised to the ITER-H98(y,2) scaling law [IPB 1999]). In these conditions, the total input power to the plasma (P_{tot}) is P_{tot} = 150 MW of which 100 MW is provided by fusion alpha particles and 50 MW by external additional heating. As mentioned above, a very high level of plasma radiation is necessary to reduce the divertor power peak power flow from the estimated ~ 20-40 MWm^{-2} for low radiation/attached divertor conditions to less than 10 MWm^{-2} as required by PFCs heat flux handling capability. The typical level of total radiated power (P_{rad}) required to achieve this in ITER is P_{rad} = 120 MW (80% of P_{tot}) with a larger contribution from the edge and divertor regions (the split being core radiation of $P_{rad,core}$ = 50 MW and edge/divertor radiation $P_{rad,div}$ =

70 MW) leading to a total plasma conducted/convected power to the divertor of ~ 30 MW or 20% of P_{tot}. Modelling of the edge plasma and edge power flow conditions expected for Q_{DT} = 10 operation in ITER shows that operation with a partially detached divertor (only the region near the separatrix is detached – evidencing pressure loss) is able to satisfy these demanding requirements regarding divertor power handling control, as shown in Fig. 1 [Kukushkin 2009], while providing appropriate He exhaust and maintaining an acceptably low core impurity contamination [Kukushkin 2009, Pacher 2010]. ITER Q_{DT} = 10 operation will take place with Be PFCs at the main wall and W PFCs at the divertor targets. For this combination of materials, intrinsic impurity radiation is not expected to sufficiently decrease the power flux to the divertor and extrinsic impurity seeding will be utilized to achieve this power flux reduction. Modelling of ITER operation with a radiative divertor with extrinsic impurity seeding satisfying the Q_{DT} = 10 requirements has so far been performed for nitrogen, neon and argon seeding [Kukushkin 2002]. With the usual definitions, the total net power flux across the separatrix ($P_{net} = P_{tot} - P_{rad,core}$) is thus P_{net} =100 MW for the ITER Q_{DT} = 10 plasma conditions. It is important to note that, for high fusion performance H-modes in ITER, the level of radiation in the main plasma is significant (~30% of P_{tot}) thus reducing the net power flux across the separatrix by 30 % compared to P_{tot}. For the plasma parameters assumed in these Q_{DT} = 10 cases, the estimated H-mode power threshold (P_{th}) is P_{th} = 76 MW [Martin 2008]. Given the sizeable level of core plasma radiation for ITER Q_{DT} = 10 conditions compared to the low levels in the experimental database (from L-modes near the H-mode transition) the value of P_{th} given above is taken to correspond to that of the edge power flow required for H-mode confinement in ITER and not to the required total input power for H-mode confinement, as one would do by direct application of the scaling on the basis of low radiation pre-H-mode L-mode plasmas. Therefore, for Q_{DT} = 10 conditions in ITER, P_{net} exceeds the H-mode threshold value of 76 MW by only about 30%.

The achievement of the required plasma confinement level (H_{98} =1) with an edge power flow only marginally exceeding the H-mode threshold power and with a radiative divertor seeded with extrinsic impurities reaching levels of total radiative fraction of ~ 80 %, as required for ITER Q_{DT} = 10, remains an unresolved research issue. Previous experiments in DIII-D had shown that radiative power fractions (~ 70-80%) and energy confinement approaching the ITER requirements (typically 10% lower than required) could be maintained by intrinsic impurity (carbon and oxygen) radiation for heating powers well above the H-mode threshold typically $P_{net}/P_{th} \geq 2$ [Petrie 1997a, Petrie 1997b, Allen 1999]. For experiments with P_{net}/P_{th} ~ 2 and with extrinsic impurity seeding (Ar), a radiated fraction of ~

60% could be achieved in DIII-D for a similar degradation of energy confinement (~10%) as in the previous experiments with intrinsic impurities [Petrie 2008]. JET and ASDEX-Upgrade experiments with extrinsic impurity seeding (N_2 and Ne, respectively) and P_{net}/P_{th} ~ 1-2 demonstrated radiated power fractions as required in ITER (70-90%) but with Type III ELMy H-mode and degraded energy confinement (H_{98} ~ 0.75 for JET) [Matthews1999, Gruber1995], although in ASDEX-Upgrade the confinement deterioration was ameliorated by the peaking of the density profile [Gruber 1995]. Experiments in Alcator C-Mod studied the compatibility of the Enhanced D-alpha H-mode regime with radiative divertor operation [Goetz 1999] by nitrogen seeding for P_{net}/P_{th} ~ 0.7 and found that radiative power fractions of ~ 90% could be achieved in H-mode with a normalised confinement H_{98} ~ 0.7. Subsequent experiments at JET with Ar and N_2 seeding explored the compatibility of a radiative divertor and Type I ELMy H-mode plasmas with $H_{98} > 0.9$ and P_{net}/P_{th} ~ 1-2 [Rapp2004, Monier-Garbet 2005]. In these experiments it was found that such conditions could be maintained up to a radiated power fraction of 60-70% (the higher end corresponding to N_2 seeding). Increasing the radiated power fraction further lead to a transition to a Type III ELMy H-mode and a further decrease of energy confinement (H_{98} = 0.7-0.8), which has been recently confirmed by systematic studies with N_2 and Ne seeding at JET [Maddison 2010]. Recent experiments in ASDEX-Upgrade with N_2 seeding have demonstrated radiated power fractions of ~ 60% with $H_{98} \geq 1.0$ at relatively high levels of input powers $P_{net}/P_{th} \geq 2$ [Tardini 2009, Schweinzer 2010]. In these experiments the high energy confinement obtained with N_2 seeding is associated with high plasma temperatures for these plasmas which is believed to be due to the influence of the seeded impurities on reducing the plasma turbulence and thus improving the energy transport [Tardini 2009, Schweinzer 2010].

This paper describes the results of a series of experiments on the Alcator C-Mod tokamak carried out to determine: a) the physics mechanisms that influence the change of plasma confinement with increasing plasma radiation, b) the possible role of divertor plasma conditions and divertor plasma detachment on the observed plasma confinement behaviour and c) to determine the dependence of the maximum radiated fraction compatible with good H-mode confinement on the atomic species dominating the radiated power.

The paper is organised as follows: section 2 describes the plasma conditions and methodology followed in the experiments, section 3 describes the results concerning plasma confinement behaviour and its relation to edge power flow and pedestal/core plasma characteristics in these experiments, section 4 describes the overall power balance and divertor plasma conditions in these experiments and their influence on plasma confinement

and finally section 5 summarises the results paper in view of their extrapolation to ITER and draws conclusions.

2. Overview of experiments in Alcator C-Mod.

Alcator C-Mod [Hutchinson 1994, Marmar 2007] is a compact, high field tokamak with vertical plate divertor geometry and RF-based heating systems (LHCD and ICRH). The experiments reported in this paper were carried out with ICRH heating of plasmas in the EDA (Enhanced D-alpha) H-mode confinement regime [Greenwald 1999]. The EDA H-mode is an ELM-less H-mode plasma in which density transport is enhanced by the presence of a quasi-coherent mode at the plasma edge which arrests the density rise typical of ELM-free H-mode and prevents impurity accumulation in the core that would otherwise lead to excessive core radiation. The quasi-coherent mode also prevents the plasma from reaching unstable edge pressure/current gradients and thus triggering edge instabilities known as ELMs. Because of the large erosion of ITER PFCs [Federici 2003] and the possible detrimental effects on plasma performance of impurity influxes produced by ELMs, the maximum loss of energy during ELMs must be significantly reduced in ITER from its expected "natural" or "uncontrolled" values by factors of ~ 30 resulting in a controlled ELM energy loss (ΔW_{ELM}) smaller than 0.2 % of the total plasma energy (W_{plasma}), which is W_{plasma} = 350 MJ for the Q_{DT} = 10 scenario [Loarte 2010]. In this respect, the EDA regime in Alcator C-Mod represents a good proxy for the controlled ELM regimes required for high fusion gain experiments in ITER.

The experiments described in this paper were carried out with a plasma current of 0.8 MA and a toroidal field of 5.4T in a diverted plasma configuration with elongation of 1.5 and upper and lower triangularities of 0.22 and 0.52 respectively, as shown in Fig. 2. All discharges were heated by ICRH and the range of total heating power (Ohmic + ICRH) into the plasma spanned the range from 2.4 – 5.0 MW. The plasma line average density in these experiments was in the range of 2.5-3.0 10^{20} m^{-3}. Regarding plasma radiation, four conditions were explored: discharges in which plasma radiation was produced by the intrinsic impurities in the Alcator C-Mod tokamak (mainly Mo and B) or by extrinsic impurities which were injected by gas puffing into the outer midplane region of the device (N_2, Ne and Ar). The experiments consisted of a series of scans in which the additional heating power, impurity seeding rate and species and plasma density (to some degree) were varied. A large variation of P_{net} by a factor of 3 was thus obtained by varying the additional heating power itself and by varying the level of impurity seeding at various levels of additional heating power. An example of several plasma discharges obtained in these experiments with different impurity

seeding species (N_2, Ne, Ar) is shown in Fig. 3. As will be described in more detail later in sections 3 and 4, Fig. 3 already shows that seeding with lower Z impurities allows the achievement of H-mode plasmas with high confinement ($H_{98} = 1$) and very low power fluxes to the outer divertor, which is well diagnosed for heat flux measurements in Alcator C-Mod [LaBombard 2010, Terry 2010].

3. Energy confinement and its relation to edge power flow and core plasma profiles.

A complete study of the factors that affect energy confinement in Alcator C-Mod including other H-mode regimes (ELMy H-mode) is the subject of a separate publication. In this section we describe the key findings obtained in these experiments with regards to the change of energy confinement with impurity seeding level and species; the reader is referred to [Hughes 2010] for a more detailed study of this topic for Alcator C-Mod. In the experiments reported in this paper, the normalised energy confinement in Alcator C-Mod has been found to be very well correlated with the edge power flow margin above the H-mode threshold as characterised by P_{net}/P_{th} as shown in Fig. 4, where P_{th} is the H-mode threshold power from the scaling for ITER-like plasmas [Martin 2008]. In addition to the values for EDA H-modes, the normalised energy confinement for some L-mode discharges carried out in the same plasma configuration as the H-mode experiments is shown for comparison in Fig. 4. The fact that the L-mode points in these experiments are found in a range of P_{net}/P_{th} for which H-mode plasma conditions are expected ($P_{net}/P_{th} \geq 1$) indicates that the scaling law used to evaluate P_{th} [Martin 2008] underestimates the power required for H-mode access in these particular experimental conditions in Alcator C-Mod (N.B. As on other devices, the actual power at the L-H transition easily can be 50% above or below that predicted by the scaling law, depending on experimental conditions). Therefore the margin of P_{net} above the power that would be required to access H-mode conditions with high reliability (for the same level of plasma density than the one obtained in the fully developed H-mode) in these experiments is actually lower than that represented by the abscissa in Fig. 4.

As shown in Fig. 4, for $P_{net}/P_{th} \geq 1$ the normalised confinement satisfies or exceeds the ITER requirements, i.e. $H_{98} \geq 1$, and is to a large degree independent of the radiating impurity (intrinsic-unseeded, N_2, Ne, Ar). For $P_{net}/P_{th} < 1$, on the contrary, a lower energy confinement is found for intrinsic (Mo and B) and Ar seeded discharges than for lower Z (N_2, Ne) seeded discharges. The dependence of H_{98} on P_{net} is mainly caused by the dependence of the normalised energy confinement in Alcator C-Mod on pedestal temperature (characterised by the electron temperature at 95% of the normalised magnetic flux $T_{e,95}$), through its influence on the core temperature through profile stiffness [Greenwald 1997], for the relatively

invariant density of EDA H-modes [Hughes 2007]. As seen in Fig. 5, this result continues to hold in seeded conditions. The differences in energy confinement engendered by injection of different Z impurities are associated with a different density behaviour; lower Z impurity seeding leads to a higher pedestal electron density (characterised by the electron density at 95% of the normalised magnetic flux $n_{e,95}$) for the same pedestal temperature, as shown in Fig. 6. The effect of injecting various impurities on the plasma density is clearer for lower pedestal temperatures, which is consistent with the larger differences in plasma confinement amongst the various injected impurities observed for lower values of $T_{e,95}$ (see Fig. 5).

The effect of changing injected impurity seeding species on the relation between energy confinement and total radiated power fraction (f_{rad}) is shown in Fig. 7. In this figure f_{rad} is derived from measurements of the power flow to the outer divertor (P_{odiv}) (which receives the highest power fluxes in these experiments) and the effective total plasma heating power ($P_{loss} = P_{tot}$-dW/dt) as $f_{rad} = (P_{loss}-P_{odiv})/P_{loss}$. Detailed discussions on the accuracy of the global power balance in these Alcator C-Mod experiments can be found in the next section. As shown in Fig. 7, higher Z impurity seeding is found to cause the largest deterioration of the energy confinement for a given level of f_{rad}. The reasons for this effect are twofold: a) for a given level of radiated power, higher Z impurity (Ar) seeding leads to larger radiated power emission from the core plasma and thus to a reduced P_{net}, which in turn reduces H_{98} and b) for a given P_{net}, H_{98} is found to be equal ($P_{net}/P_{th} \geq 1$) or lower ($P_{net}/P_{th} \leq 1$) for higher Z impurity (Ar) seeding as compared to lower Z impurity (N_2, Ne). In this respect, N_2 is found to be optimum for Alcator C-Mod to achieve the highest levels of radiated power while maintaining good H-mode confinement. With N_2 seeding, radiated power fraction levels of 95% can be reached in Alcator C-Mod while maintaining $H_{98} = 1$ thus exceeding two of the crucial requirements for ITER $Q_{DT} = 10$ operation.

Contrary to results in other experiments [Gruber 1995], the high energy confinement achieved with low Z seeding in Alcator C-Mod is not associated with the peaking of density profiles. This is shown in Fig. 8 for three discharges with similar pedestal (and core plasma) temperatures and deuterium fuelling with Ar, Ne or N_2 seeding, respectively. While the electron density is highest for N_2 seeding, thus leading to higher energy confinement, the shape of the profile itself is similar to that of Ar or Ne showing that the enhanced confinement with N_2 is associated with the increase of the density and not of its peaking. One possible reason for the lack of peaking of the density profiles is that Alcator C-Mod uses central heating by ICRH which has been proven to prevent density peaking and impurity

accumulation in several tokamaks through its effect on anomalous particle transport (see, for instance, [Stober 2003]).

The increase in plasma electron density appears to be more than that which would be associated with an increased impurity concentration. The measured average Z_{eff} of these discharges is highest for the lowest Z seeding; Z_{eff} = 2.4 (Ar), 2.3 (Ne) and 3.1 (N_2). The corresponding neutron rate produced by DD fusion reactions (N_{DD}) increases by more than 50% when comparing the lowest and the highest Z impurity seeded discharge N_{DD} ($10^{13}s^{-1}$) = 5.0 (Ar), 4.4 (Ne) and 8.1 (N_2). As the temperature of these discharges is similar (see Fig. 8), this neutron rate increase requires a corresponding increase of the deuterium density as $n_D \propto \sqrt{N_{DD}}$. This corresponds to a deuterium density increase of 27 % from the Ar to the N_2 seeded discharge, which is virtually the same as the electron density ratio between these two discharges. Neutron production in Alcator C-Mod, which does not have NBI heating, is dominated by the hottest/central region of the plasma and, thus, a direct evaluation of the resulting core impurity density by combining these measurements with those of the average Z_{eff} is not possible. It is therefore not possible to make a conclusive statement regarding how much of the increase in electron density with N_2 seeding is caused by the increased deuterium density and by the increased impurity density. However, the available evidence indicates that N_2 seeding in Alcator C-Mod leads to a particle transport improvement for the main plasma ions in these EDA H-mode experiments. The evaluation of the consequences of impurity seeding with regards to the increase of the core impurity density is very important for ITER, as it affects the reactivity of the fusion plasma and it will discussed in more detail in section 5.

4. Divertor plasma characteristics and relation to energy confinement.

Characterisation of the divertor plasma conditions in these experiments has been carried out by means of Langmuir probes embedded in the divertor target, visible and VUV spectroscopy, bolometer cameras integrating the radiation emission along several chords viewing the divertor region and the core plasma and measurements of the power/energy fluxes to the divertor by the infrared cameras and embedded thermocouples. A detailed description of divertor power flow measurements and diagnostics for Alcator C-mod can be found in [LaBombard 2010, Terry 2010]; for radiated power measurements and diagnostics the reader is referred to [Reinke 2010]. For the type of studies discussed in this paper, which deal with the absolute magnitude of the edge power flow and the amount of power which is radiated versus the total input power, it is important to assess the accuracy of the power measurements. This has been assessed by comparing the total input power with measurements

of the power radiated from the core and divertor plasmas plus that measured at the outer divertor target. As shown in Fig. 9 the agreement between both estimates is reasonably good within ± 20%, although at high levels of total power (and divertor radiated power) more power is estimated from the losses than from the plasma heating power for N_2 seeded discharges. This is believed to be in part associated with the overestimate of the diverted radiated power associated with neutral fluxes arriving at the bolometers, which has been found to lead to an overestimation of the divertor radiation by as much as 10% in previous experiments with N_2 seeding in Alcator C-Mod [Goetz 1999]. Similarly, for very high radiation conditions it is possible that a fraction of the divertor radiated power is deposited at the outer divertor target and thus being accounted twice in the global power balance. For high divertor radiation conditions this is a possible effect which has already been identified in other experiments [Herrmann 2002, and references therein] and in the simulations for ITER shown in Fig. 1. The magnitude of this effect depends strongly on the spatial distribution of the radiation emissivity and on its proximity to the divertor target, both influencing the solid angle for radiation deposition at the divertor target, as well as on the reflectance of the divertor target surface in the wavelengths dominating the electromagnetic radiation emission by the plasma. A quantitative estimate of the effect requires high resolution tomographic reconstructions which are not feasible for these experiments in Alcator C-Mod. However, simple estimates carried out on the basis experimental evidence from nitrogen emission in UV (see Fig. 13 for an example) indicates that the effect for these Alcator C-Mod conditions is not large (~ 30% for peak heat flux and total divertor flux), because in these experiments the radiation peak is located near the X-point and thus not close to the outer strike zone, as it is the case in the ITER simulation in Fig. 1 for which radiated power redeposition is large. Although no infrared-camera measurements of power deposited on the inner divertor in Alcator C-Mod exist, Langmuir probe measurements indicate the power flux to the inner divertor is low for these discharges. Similarly, measurements of the integral energy deposition to the limiters in the main chamber show that typically less than 20% of the total injected energy into the plasma is measured at the limiters, which is consistent with the 20% maximum error bar for the global power balance shown in Fig. 9, part of which is also expected to be associated with the deposition of the power radiated by the plasma in the main chamber.

Taking into account the uncertainties above, it is thus possible to produce a similar analysis of the energy confinement dependence on the radiated power fraction based on bolometric measurements and to compare it with the evaluation in Fig. 7, which is shown in

Fig. 10. Consistent with the results of Fig. 9 and the discussion above, for the highest radiated power levels with N_2 seeding, the radiated power fraction as determined by bolometric measurements exceeds unity while plasma confinement remains good (H_{98} ~ 1). Besides highlighting the difficulties of accurately measuring the divertor radiated power in conditions with high radiation level and detachment, the results in Fig. 10 indicate that the approach followed in Fig. 7 provides a reasonably accurate lower estimate for the radiated power fraction for these experiments.

Increasing the level of radiated power in the core and divertor plasma by impurity seeding causes a substantial decrease of the power flux deposited by the plasma at the outer divertor. The largest decrease occurs when the outer divertor plasma approaches the partially detached divertor regime. The decrease of the peak power flux at the outer divertor target can be as large as a factor of 6 for lower Z impurity seeding (N_2, Ne) when compared to attached unseeded discharges with similar levels of edge power flow, as shown in Fig. 11. This level of reduction of the peak power flux carried by the plasma is similar to that required for ITER operation in the $Q_{DT} = 10$ regime (see Fig. 1). As is also shown in Fig.11, the reduction of the divertor peak heat flux as required for ITER is compatible with maintaining a good energy confinement $H_{98} \geq 1$ with P_{net}/P_{th} ~1 for low Z impurity seeding in Alcator C-Mod. Further evidence of detached divertor plasma conditions at the outer divertor is shown in Fig. 12 where Langmuir probe measurements show that the electron temperature decreases from values near the separatrix of 20-30 eV, for unseeded and Ar seeded discharges (values typical of attached divertor plasmas), to a few eV for Ne and N_2 seeding (typical of detached plasmas).

The compatibility between detached divertor plasmas and H-modes with high energy confinement with H_{98} ~ 1 has been further investigated by analysis of the radiation emission by nitrogen ions in the UV range. In agreement with previous experiments in Alcator C-Mod and other devices [Petrie 1997, Petrie 2008, Matthews 1999, Gruber 1995, Monier-Garbet 2005, Goetz 1999], Fig. 13 shows that the radiation emissivity for the N^{4+} line (124 nm) develops a strong peak in the vicinity of the X-point with increasing divertor radiated power levels. Spatial profiles of visible N^+ and N^{2+} emission, not shown, are also peaked near the X-point but have broader profiles in the region under the X-point than those of N^{4+} shown in Fig. 13. Although measurements in Alcator C-Mod are insufficient to evaluate the contribution of nitrogen in general, and of this ion charge state in particular, to the total radiation, previous experiments at JET have shown that for detached plasma conditions with nitrogen seeding, up to 80% of the observed divertor radiation can be accounted by VUV

emission by nitrogen with N^{4+} being the dominant radiator (about 40% of the radiation emitted by nitrogen was attributed to this ionic species) [Maggi 1997].

It has been frequently speculated that detachment of the divertor plasma and the migration of the radiation peak to the vicinity of the X-point are responsible for the deterioration of confinement found in previous radiative divertor experiments. This is thought to occur either because of direct radiation cooling of the edge plasma or by the deteriorated neutral compression in the divertor that is associated with plasma detachment and the subsequent negative effects of the escaping divertor neutrals on plasma confinement [Rapp 2004, Monier-Garbet 2005, Rapp 2009, Petrie 1997a, Petrie 1997b]. Consistent with this physics picture, detachment of the divertor and movement of the radiation to the X-point has been developed as one criterion defining the operational limits of the ITER divertor with high confinement plasmas [Kukushkin 2009]. The results of the current study in Alcator C-Mod, for which $P_{net}/P_{th} \sim 1$, generally contradict the association of X-point radiation and divertor detachment with poor energy confinement. While the X-point radiation was high for N_2 seeding (Fig. 13) and the peak divertor heat flux and outer divertor electron temperature reached values corresponding to partial detachment (Figs. 11 and 12), these conditions are clearly compatible with a high temperature/high confinement plasma (T_{ped} = 450 eV in the discharge shown in Fig. 13) if the edge power flow is maintained at a sufficiently high level ($P_{net}/P_{th} \geq 1$). As also shown in Fig. 13 (where the measured electron temperature profiles at the midplane have been mapped along the sightlines of the VUV chord integrated measurements), the large flux expansion near the X-point region provides an effective separation in real space between the regions of high radiative power densities and the pedestal plasma. For this reason, most of the radiated losses that occur near the X-point in this very highly radiative divertor are actually originated from flux surfaces in the very outer regions of the confined plasma and the SOL (1-2 mm inside the separatrix mapped to the outer midplane) and thus have little effect on the top of the pedestal plasma parameters, which are located further inside the plasma and, consequently, on the H-mode confinement quality.

It is important to note that in these experiments the midplane N_2 gas puff valve, at high injection rates, was open for the entire H-mode phase of the discharge without any feedback during the discharge (see Fig. 3). It is possible that further optimisation of the plasma confinement versus radiative power fraction can be achieved with a well-controlled N_2 injection and seeding from the divertor region. This would allow a more detailed study of the relation between plasma confinement, X-point radiation characteristics (magnitude and profiles) and the level of N_2 injection. These studies are closely related to the poorly

understood question of how stable and controllable the detachment front and divertor radiation location will be in a machine like ITER.

5. Summary and Conclusions.

The results obtained in the Alcator C-Mod experiments described in this paper have provided for the first time an experimental demonstration of radiative divertor operation meeting or exceeding the requirements of both a sufficient reduction of the divertor power load ($P_{odiv}/P_{loss} \leq 0.2$) while maintaining a sufficient energy confinement ($H_{98} \geq 1$) with an edge power flux marginally exceeding the L-H transition power ($P_{net}/P_{th} \sim 1$) as shown in Fig. 14. This has been achieved with "standard" core plasma density profiles, that is without enhanced plasma density peaking unlike in previous experiments [Gruber 1995]. This, by itself, is a major achievement in this field of research although some aspects of the extrapolation from Alcator C-Mod to ITER are non-trivial.

The major result obtained in these experiments which is directly extrapolable to ITER is the demonstration of the role of the edge power flow in determining the plasma pedestal parameters and plasma confinement independently of divertor plasma conditions. Alcator C-Mod experiments with ITER-like edge power flows with $1.0 \leq P_{net}/P_{th} \leq 1.4$ have demonstrated that H-modes with normalised energy confinement $H_{98} \geq 1$, together with an outer divertor total power load as low as ~ 5% of the total input power and a partially detached outer divertor can be obtained with N_2 seeding. An important issue to clarify is what aspects of the behaviour observed in Alcator C-Mod are associated with the experiments being performed in the EDA regime as opposed to others performed in the Type I ELMy H-mode regime, which showed transitions to the Type III ELMy H-mode regime at very high radiation levels and large confinement drops [Matthews 1999, Rapp 2004, Monier-Garbet 2005, Rapp 2009]. In this respect, it is important to note that for the lowest P_{net} levels in these experiments with $H_{98} \sim 0.8$ and low pedestal temperature, Type III ELM-like activity is also found in Alcator C-Mod so that the EDA H-mode regime in this sense may be analogous to the Type I ELMy H-mode in other devices. This, together with the stringent requirements associated with the control of Type I ELM energy losses in ITER [Loarte 2010], supports the contention that the EDA H-mode experiments described in this paper are a good proxy to reproduce the conditions of controlled ELM regimes in ITER, in which small ELM energy losses with high pedestal energy need to be maintained.

Therefore, the major open issue for extrapolating these Alcator C-mod results to ITER is associated with the levels of divertor radiated power and associated impurity densities. This is a non-trivial extrapolation as the level of divertor radiation and edge and core impurity

density are influenced by divertor plasma parameters, dimensions/geometry and SOL and pedestal plasma parameters which are expected to be very different in ITER from those in Alcator C-Mod. Thus, a proper extrapolation of the magnitude and distribution of the radiative losses from Alcator C-Mod to ITER requires detailed edge plasma-impurity-neutral modelling which is itself subject to significant uncertainties (plasma anomalous transport, flows along the field, detachment processes, etc.), and is beyond the scope of this paper. A simpler approach to provide some insight into this issue is to compare the measured Z_{eff} with the total radiated power by application of an existing scaling for radiative plasma conditions from a multi-machine database [Matthews 1997]. Application of this scaling to ITER Q_{DT} = 10 operation with Ne seeding to achieve a total radiated power of 120 MW provides an expected value for Z_{eff} = 2.0, which is already somewhat larger than that obtained by edge modelling for ITER, for which Z_{eff} = 1.6 excluding the He contribution from alpha particles [Kukushkin 2002]. Comparing the measured Z_{eff} in the current Alcator C-Mod experiments with the expectations from this scaling shows that the measured value exceeds significantly the expected value from the scaling, as shown in Fig. 15. For comparison, Fig. 15 also shows results obtained in previous nitrogen seeded EDA H-modes [Goetz 1999] which had values of Z_{eff} much closer to the scaling, albeit with a deteriorated energy confinement H_{98} ~ 0.7. The higher impurity concentration in the present set of radiative divertor experiments with higher confinement compared to the previous ones is a result of various factors : a) the goal of the present experiments was to study the interplay between edge power flow, divertor conditions and plasma confinement and no attempt to optimise the impurity seeding to minimise Z_{eff} was made, b) the impurity seeding in these experiments was performed by midplane puffing unlike the previous experiments for which divertor impurity puffing was used; impurity penetration into the core plasma from the midplane is know to be much larger than from the divertor and, in this sense, the experiments presented in this paper were "de-optimised" for impurity contamination of the main plasma, c) in order to explore an appropriate range of P_{net}/P_{th} the present experiments were carried out at reduced current of 0.8 MA and moderate line average density of ~ 3.0 10^{20} m^{-3}, compared to ~ 5.0 10^{20} m^{-3} in the previous experiments with deteriorated energy confinement. Given the scaling of radiated power as $P_{rad} \sim (Z_{eff}-1) \times n_e^2$, this difference in density alone is sufficient to explain a large fraction of the increase in Z_{eff} in the new experiments (typically Z_{eff} = 2.5-3.5) compared to the previous ones (typically Z_{eff} = 1.8) and d) the present experiments have been mainly carried out at higher level of heating powers than in the previous experiments; thus even if the radiated power fractions are similar the absolute magnitude of the radiated power is larger in the newer experiments

(typically 4-5 MW compared to less than 4 MW in the previous experiments), requiring a higher level of impurity density.

In order to resolve the outstanding issues regarding the extrapolability of the results obtained in Alcator C-Mod to ITER with a view to demonstrate a fully integrated scenario for Q_{DT} = 10 operation with regards to confinement, edge power flow, divertor heat flux control and core plasma impurity contamination, a new series of experiments will be performed. These new experiments will focus on the optimisation of the core plasma impurity contamination for a given radiative power fraction by adjustment of the plasma density and impurity gas puffing waveform and injection location in EDA H-modes. To study the effect of ELMs on the interplay between confinement and edge power flow at, or just above, the expected L-H transition power threshold, an expanded set of experiments in ELMy H-modes with impurity seeding in Alcator C-Mod will also be carried out.

Acknowledgements

The authors would like to thank the Alcator C-Mod operations staff for their contribution to the success of the experiments reported in this paper and to A. Kukushkin for providing the results of ITER modelling and Fig.1. This work was supported by the US Department of Energy Agreement DE-FC02-99ER54512.

Disclaimer

The views and opinions expressed herein do not necessarily reflect those of the ITER Organization.

6. References.

[Allen 1999] Allen, S.L., et al., Nucl. Fusion **39** (1999) 2015.

[Federici 2003] Federici, G. et al., Plasma Phys. Control. Fusion (1993) **45** 1523.

[Goetz 1999] Goetz, J.A., et al., Phys. Plasmas **6** (1999) 1899.

[Greenwald 1997] Greenwald, M., et al., Nucl. Fusion **37** (1997) 793.

[Greenwald 1999] Greenwald, M., et al., Phys. Plasmas **6** (1999) 943.

[Gruber 1995] Gruber, O., et al., Phys. Rev. Lett. **74** (1995) 4217.

[Herrmann 2002] Herrmann, A., Plasma Phys. Control. Fusion **44** (2002) 883.

[Hughes 1997] Hughes, J.W., et al., Nucl. Fusion **47** (2007) 1057.

[Hughes 2010] Hughes, J.W., et al., Proc. 23rd IAEA Fusion Energy Conference, Daejon, Korea, 2010, EXC/P3-06, submitted to Nucl. Fusion.

[Hutchinson 1994] Hutchinson, et al., Phys. Plasmas **1** (1994) 1511.

[IPB 1999] ITER Physics Basis, Nucl. Fusion **39** (1999) 2391.

[Kukushkin 2002] Kukushkin, A.S., et al., Nucl. Fusion **42** (2002) 075008.

[Kukushkin 2009] Kukushkin, A.S., et al., Nucl. Fusion **49** (2009) 075008.

[LaBombard 1995] LaBombard, B., et al., Phys. Plasmas **2** (1995) 2242.

[LaBombard 2010] LaBombard, B., et al., Bull. APS, 52nd An. Meet. Div. Plasma Phys., Volume 55, Num.15, JI2.00005.

[Loarte 1998] Loarte, A., et al., Nucl. Fusion **38** (1998) 331.

[Loarte 2008] Loarte, A., et al., Proc. 22nd IAEA Fusion Energy Conf., 13-18 October 2008, Geneva, Switzerland, paper IT/P6-13.

[Loarte 2010] Loarte, A., et al., Proc. 23rd IAEA Fusion Energy Conference, Daejon, Korea, 2010, ITR/1-4.

[Maddison 2010] Maddison, G., et al. Proc. 19th PSI Conference, San Diego, USA, 2010. Accepted for publication in J. Nuc. Mat.

[Maggi 1997] Maggi, C.F., et al., J. Nuc. Mat. **241-243** (1997) 414.

[Marmar 2007] Marmar, E.S. et al. Fusion Sci. Technol. **51** (2007) 261.

[Martin08] Martin, Y., et al., J. Phys. Conf. Series **123** (2008) 012033.

[Matthews 1997] Matthews, G.F., et al., J. Nuc. Mat. **241-243** (1997) 450.

[Matthews 1999] Matthews, G.F., et al., Nucl. Fusion **39** (1999) 19.

[Monier-Garbet 2005] Monier-Garbet, P., et al., Nucl. Fusion **45** (2005) 1404.

[Pacher 2010] Pacher, H.S., et al. Proc. 19th PSI Conference, San Diego, USA, 2010. Accepted for publication in J. Nuc. Mat.

[Petrie 1997a] Petrie, T., et al., Nucl. Fusion **37** (1997) 321.

[Petrie 1997b] Petrie, T., et al., Nucl. Fusion **37** (1997) 643.

[Petrie 2008] Petrie, T., et al., Nucl. Fusion **48** (2008) 045010.

[PIPB 2007] Progress on ITER Physics Basis, Nucl. Fusion **47** (2007) S203.

[Rapp 2004] Rapp, J., et al., Nucl. Fusion **44** (2004) 312.

[Rapp 2009] Rapp, J., et al., Nucl. Fusion **49** (2009) 095012.

[Reinke 2010] Reinke, M.L., et al. Proc. 19th PSI Conference, San Diego, USA, 2010. Accepted for publication in J. Nuc. Mat.

[Schweinzer 2010] Schweinzer, J., et al., Proc. 23rd IAEA Fusion Energy Conference, Daejon, Korea, 2010, EXC/P2-07.

[Stober 2003] Stober, J., et al., Nucl. Fusion **43** (2003) 1265.

[Tardini 2009] Tardini, G., et al., Proc.36th EPS Conference on Plasma Phys. Sofia, Bulgaria, 2009, ECA Vol.33E, O-2.004.

[Terry 2010] Terry, J.L., et al., Rev. Sci. Instrum. **81** (2010) 10E513.

Figure 1.

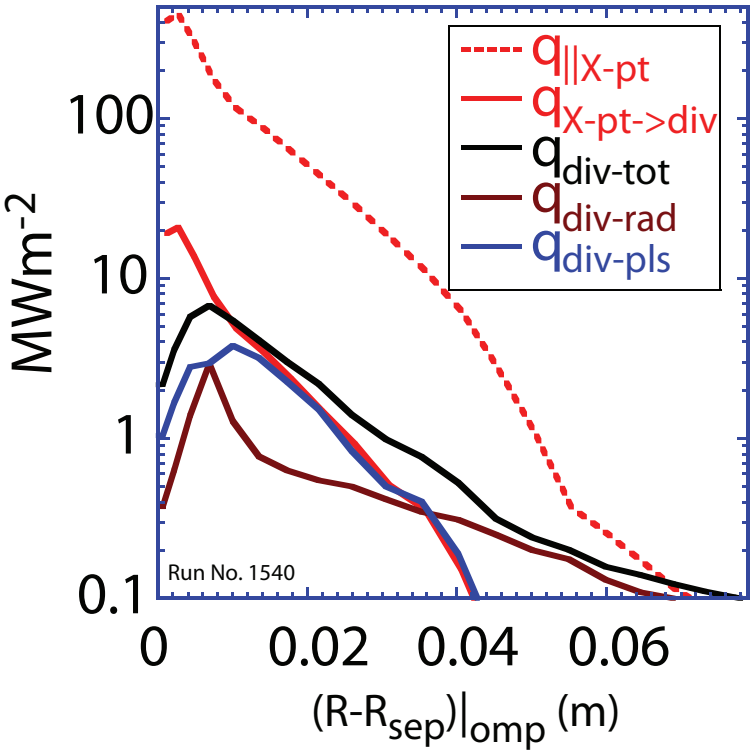

Figure 1. Modelled power flux entering the divertor and deposited onto the divertor target for typical Q_{DT} = 10 conditions in ITER [Kukushkin 2009] : $q_{\|x\text{-}pt}$ is the parallel plasma power flux entering the divertor along the field line, $q_{x\text{-}pt\rightarrow div}$ is the projection of $q_{\|x\text{-}pt}$ onto the divertor target normal to the surface, $q_{div\text{-}tot}$ is the total perpendicular power flux deposited onto the divertor by both the plasma in contact with the divertor target ($q_{div\text{-}pls}$) and by deposition of electromagnetic radiation ($q_{div\text{-}rad}$). For typical conditions in ITER, radiation in the divertor decreases the peak power flux carried by the plasma by a factor of ≥ 5 from that entering the divertor target. The total peak heat flux is reduced by a smaller amount (~ 3 - 4) due to the deposition of some of the radiated power onto the divertor target.

Figure 2

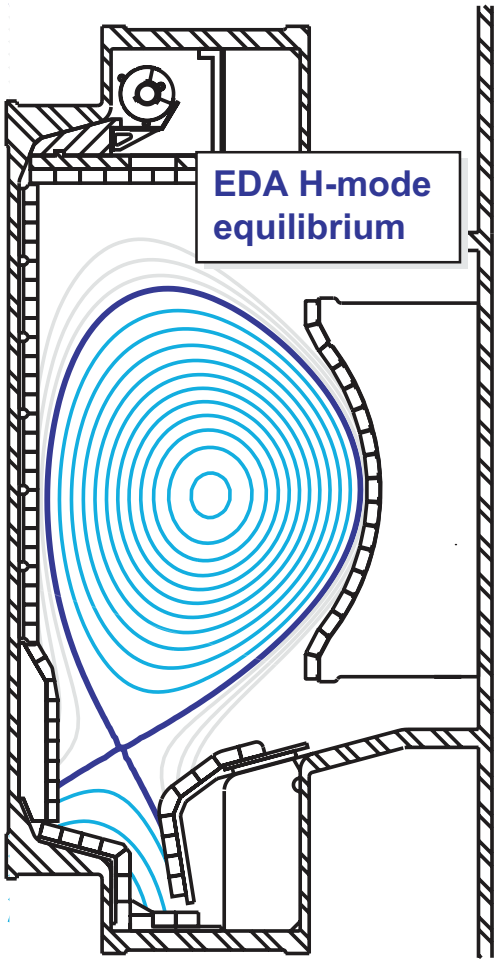

Figure 2. Plasma equilibrium reconstruction for the EDA H-mode discharges described in this paper.

Figure 3

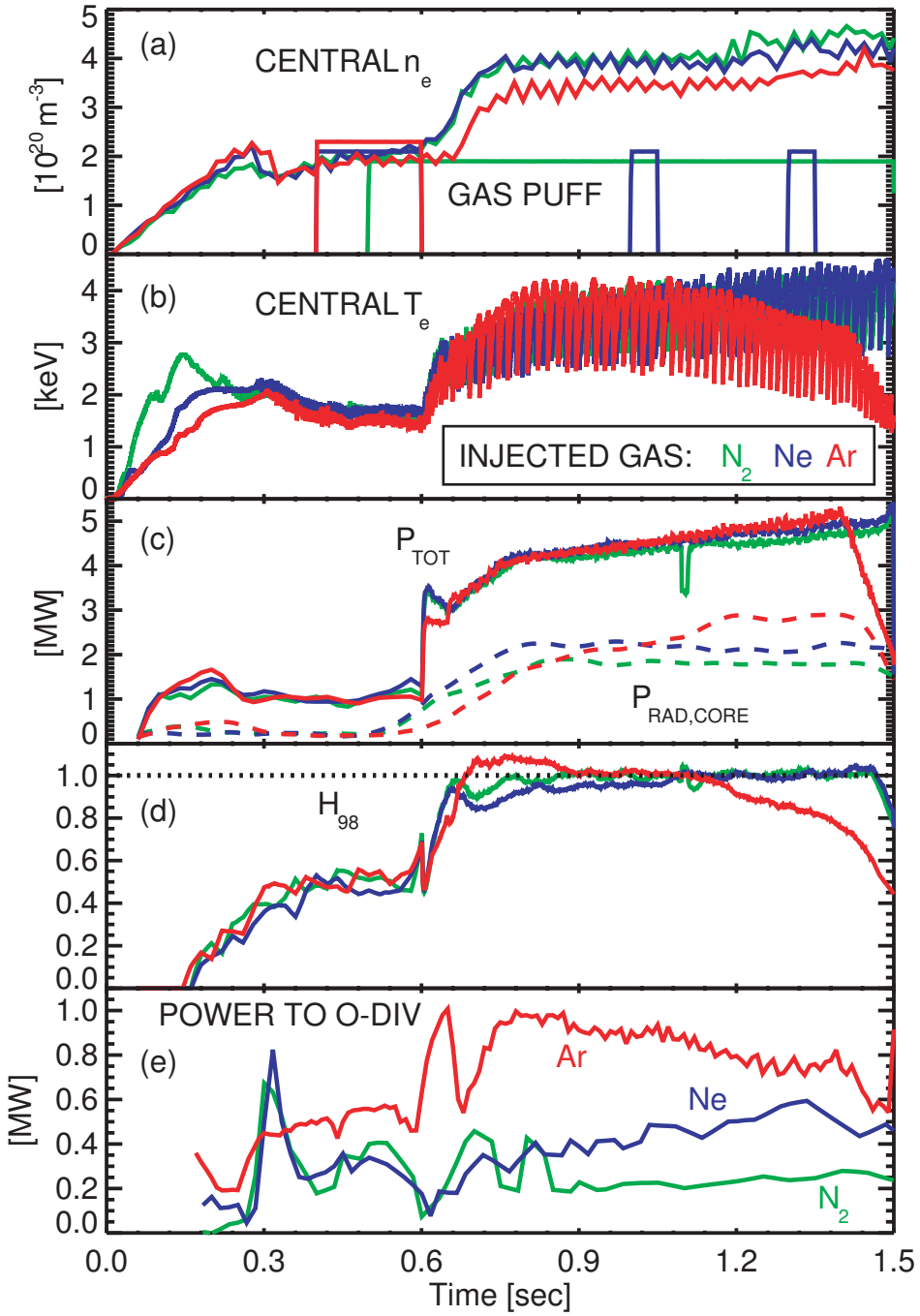

Figure 3. Typical plasma parameters for the impurity seeded EDA H-modes discharges considered in this study versus time. From top to bottom : a) central electron density and waveforms of the seeded impurities (N_2, Ne, Ar), b) central electron temperature, c) Plasma total input power (Ohmic + ICRH) and radiated power in the plasma core, d) Normalised energy confinement (H_{98}) and e) Measured power to the outer divertor target.

Figure 4

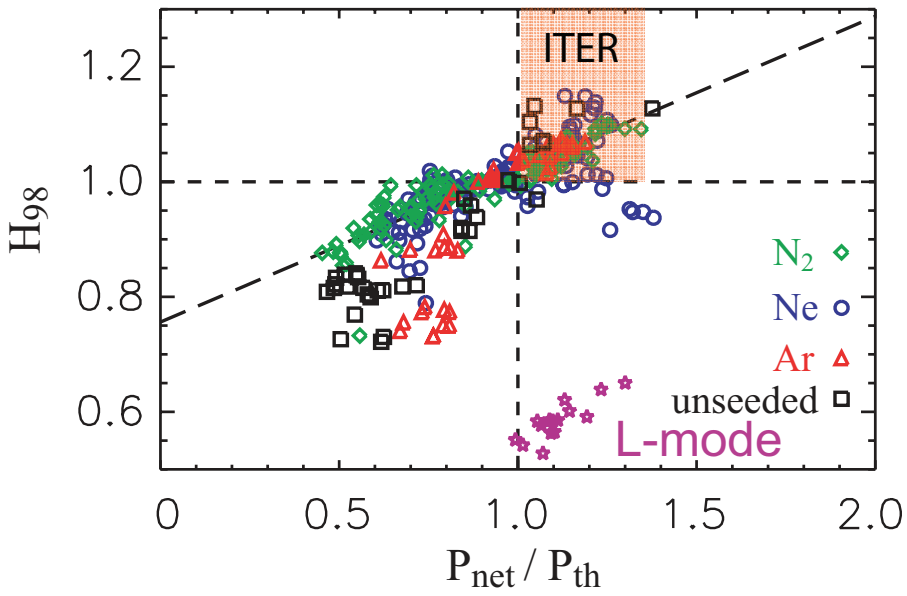

Figure 4. Normalised energy confinement versus net power crossing the separatrix (P_{net}) normalized to the H-mode threshold power (P_{th}) for EDA H-modes in Alcator C-Mod with extrinsic impurity seeding (N_2, Ne, Ar) and with intrinsic impurities (unseeded). The normalised energy confinement in L-mode discharges is shown for comparison.

Figure 5.

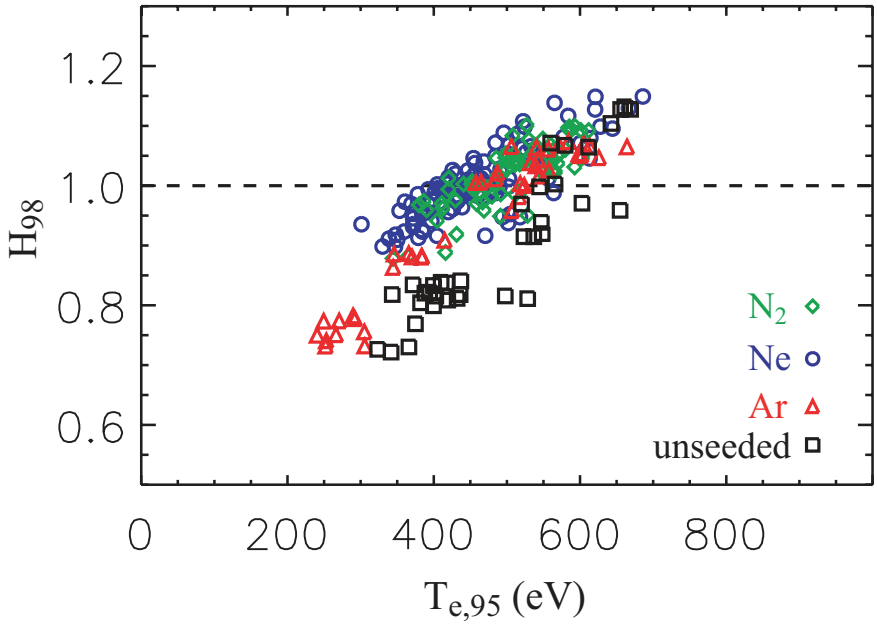

Figure 5. Normalised energy confinement versus pedestal electron temperature for EDA H-modes in Alcator C-Mod with extrinsic impurity seeding (N_2, Ne, Ar) and with intrinsic impurities (unseeded).

Figure 6.

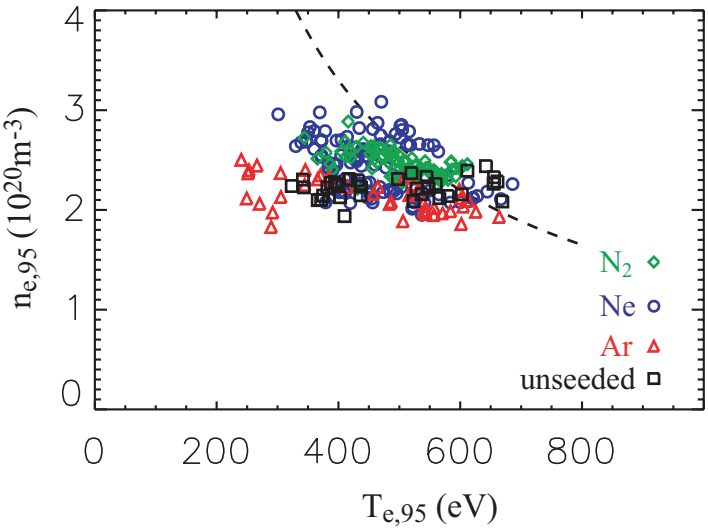

Figure 6. Pedestal electron density versus pedestal electron temperature for EDA H-modes in Alcator C-Mod with extrinsic impurity seeding (N_2, Ne, Ar) and with intrinsic impurities (unseeded) showing that for the same pedestal temperature low Z impurity seeded H-modes have higher pedestal densities.

Figure 7.

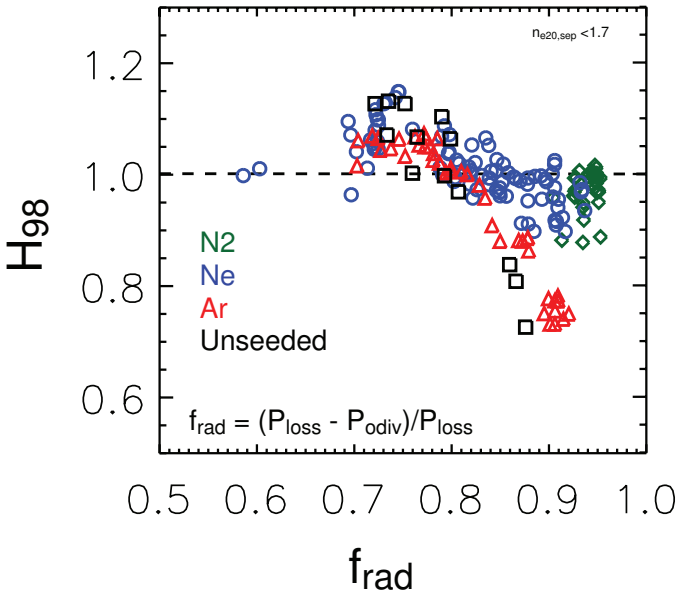

Figure 7. Normalised energy confinement versus radiated power fraction, as estimated from measurements of heating power and power flow to the outer divertor target for EDA H-modes in Alcator C-Mod with extrinsic impurity seeding (N_2, Ne, Ar) and with intrinsic impurities (unseeded) showing a higher energy confinement for low Z impurity seeded H-modes for a given radiated fraction level.

Figure 8.

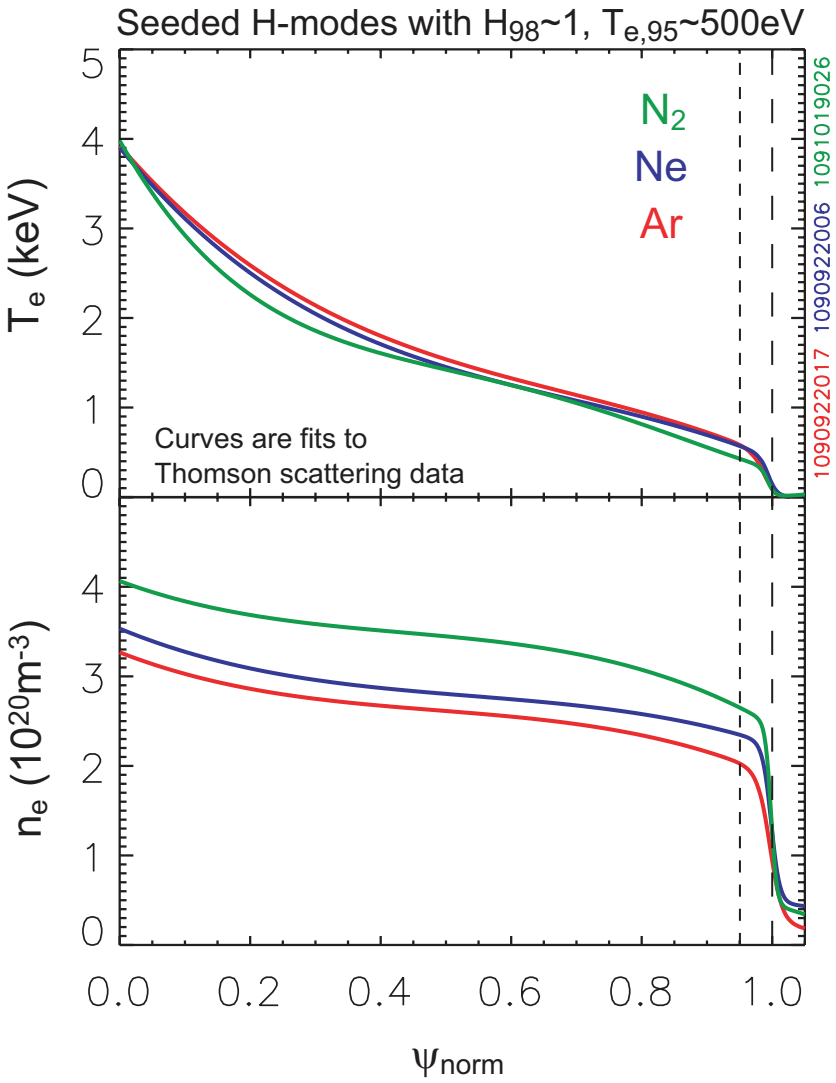

Figure 8. Electron plasma density and temperature profiles in EDA H-modes in Alcator C-Mod with extrinsic impurity seeding (N_2, Ne, Ar) versus normalised poloidal flux for discharges with similar pedestal temperatures.

Figure 9.

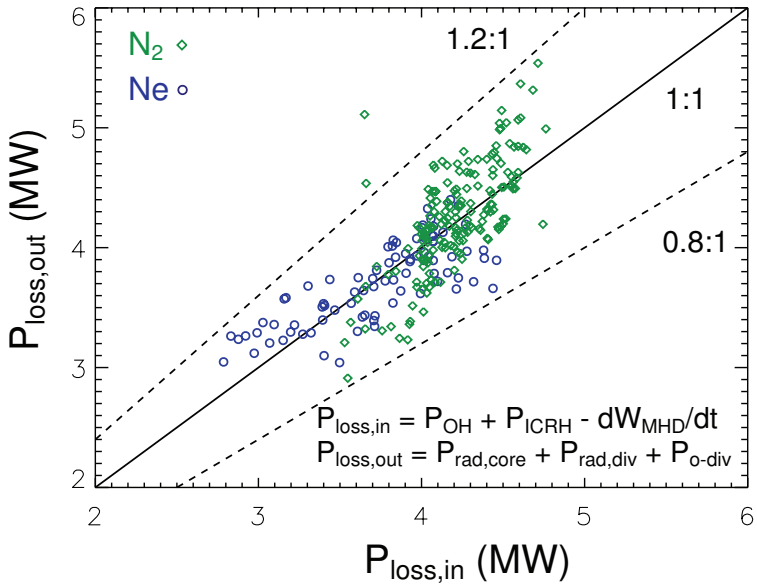

Figure 9. Measured power exhausted ($P_{loss,out}$) by the plasma by conduction/convection to the divertor and electromagnetic radiation for N_2 and Ne seeded discharges versus the effective total input power into the plasma ($P_{loss,in}$). The lines 1:1 and those corresponding to the ± 20% error are shown for comparison.

Figure 10.

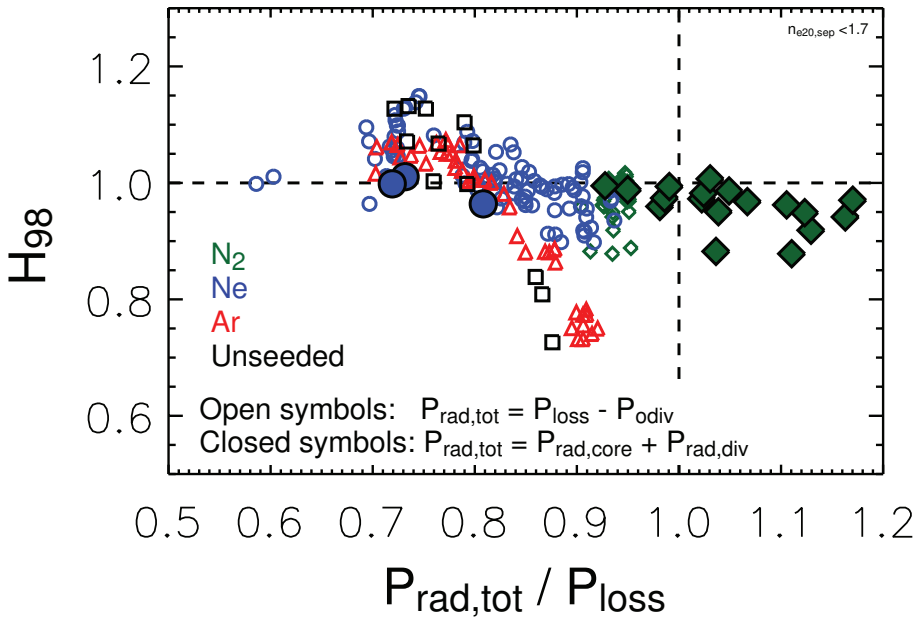

Figure 10. Normalised energy confinement versus radiated power fraction, as estimated from measurements of heating power and power flow to the outer divertor target (open symbols) and radiated power measurements (closed symbols) for EDA H-modes in Alcator C-Mod with extrinsic impurity seeding (N_2, Ne, Ar) and with intrinsic impurities (unseeded).

Figure 11.

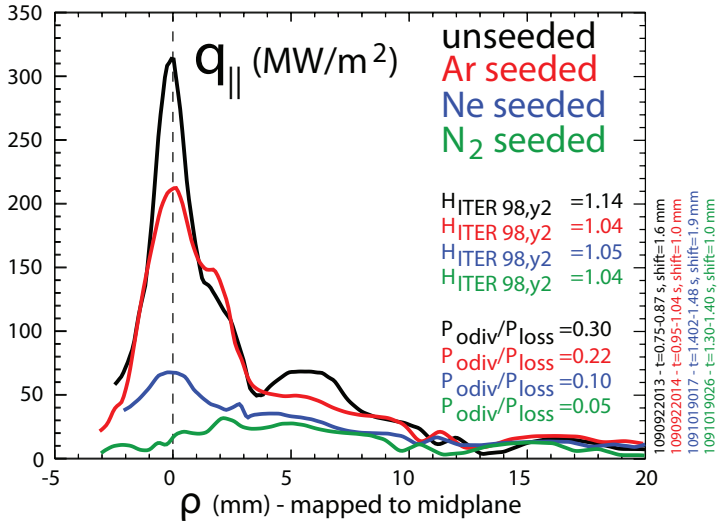

Figure 11. Measured parallel heat flux at the outer divertor target versus distance to the separatrix mapped to the outer midplane for a series of discharges with impurity seeding and similar normalised energy confinement showing the large decrease of the peak heat flux and the total power deposited at the outer divertor with decreasing Z of the seeded impurity. The net power normalised to the H-mode threshold power for these discharges is P_{net}/P_{th} = 1.10 (unseeded), 0.93 (Ar), 0.97 (Ne) and 1.0 (N_2).

Figure 12.

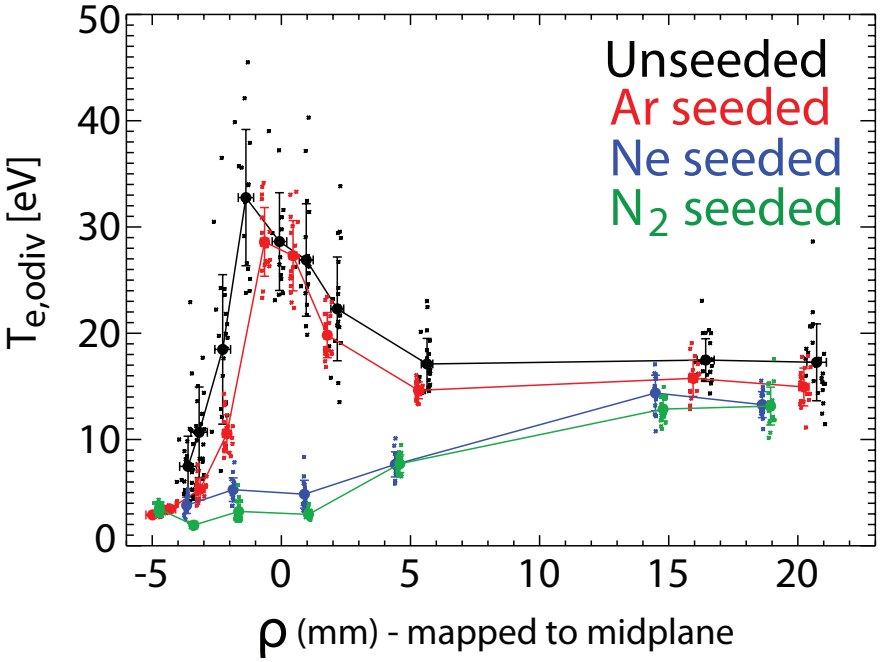

Figure 12. Measured electron temperature at the outer divertor target versus distance to the separatrix mapped to the outer midplane for the same discharges as in Fig. 11 showing the achievement of very low plasma temperatures at the divertor for low Z (N_2 and Ne) seeding.

Figure 13.

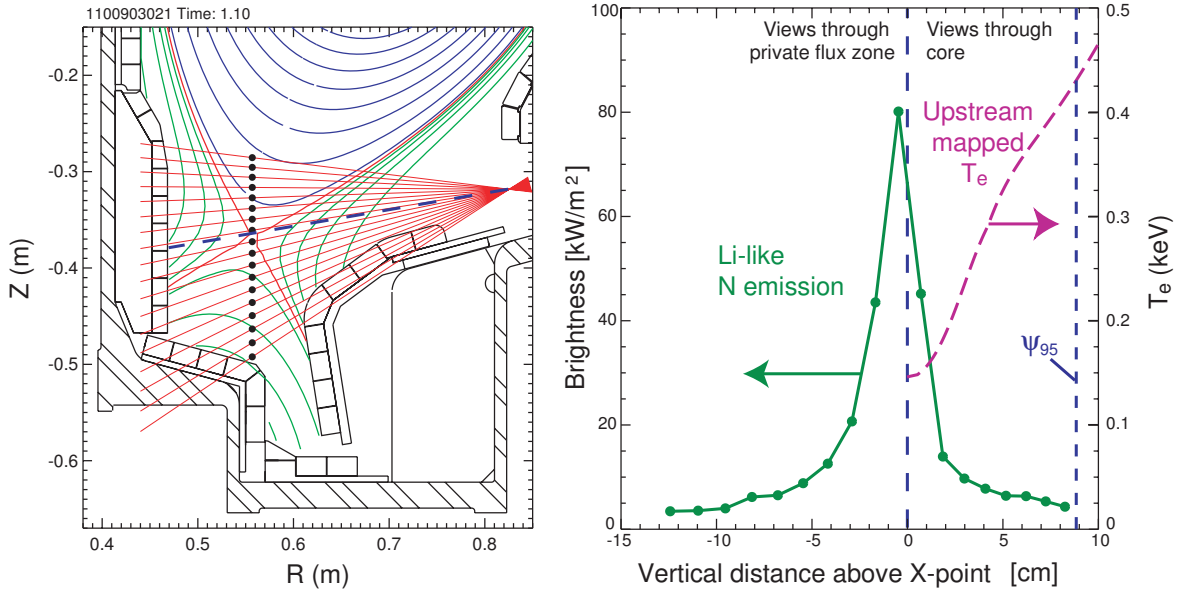

Figure 13. Measured VUV emission by N^{4+} (124 nm) along various chords in the divertor region of Alcator C-Mod for a N_2 seeded EDA H-mode showing the large peak of emission near the X-point. The electron temperature profiles measured at the midplane mapped to the divertor are shown for comparison. For this discharge H_{98} ~1 and P_{net}/P_{th} ~ 1.

Figure 14.

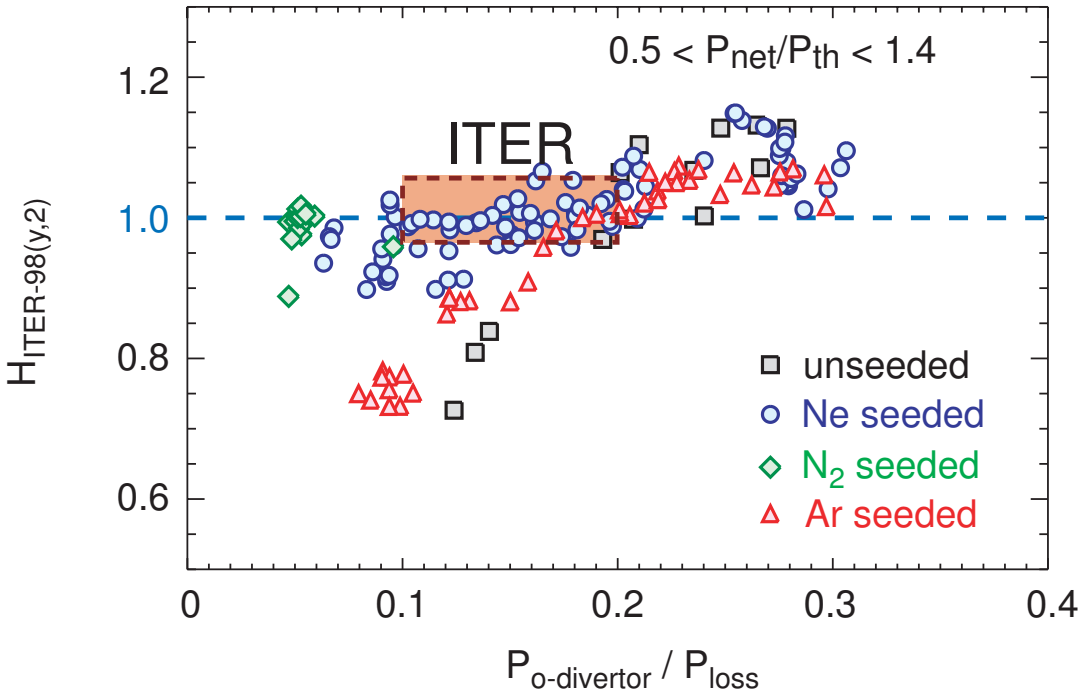

Figure 14. Normalised energy confinement versus normalised power to the outer divertor for EDA H-modes in Alcator C-Mod with extrinsic impurity seeding (N_2, Ne, Ar) and with intrinsic impurities (unseeded). The typical range expected for ITER Q_{DT}=10 operation is shown for comparison.

Figure 15.

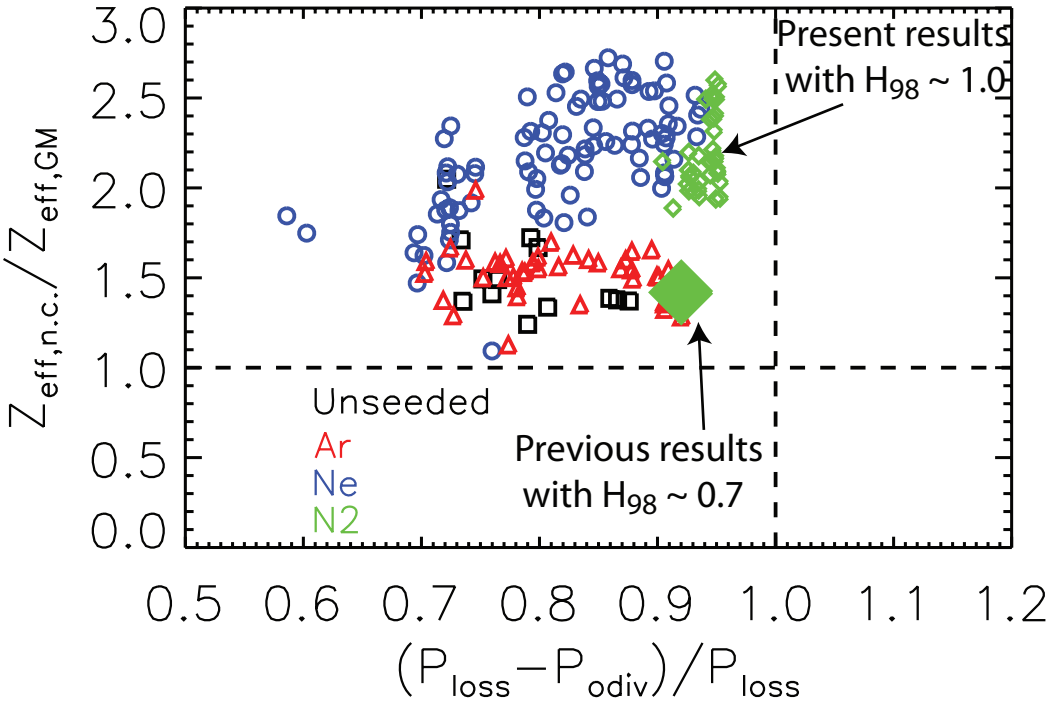

Figure 15. Ratio of the measured Z_{eff} in the EDA H-modes in Alcator C-Mod with extrinsic impurity seeding (N_2, Ne, Ar) and with intrinsic impurities (unseeded) to the Z_{eff} multimachine scaling in [Matthews 1997] versus radiated power fraction. The value for the previous nitrogen seeded radiative EDA H-modes in Alcator C-mod with deteriorated confinement is shown for comparison [Goetz 1999].